

Simulation study on CFRP strengthened reinforced concrete beam under four-point bending

Dongliang Zhang^{1a}, Qingyuan Wang^{*1,2} and Jiangfeng Dong¹

¹College of Architecture and Environment, Sichuan University, Chengdu 610065, China

²Failure Mechanics and Engineering Disaster Prevention and Mitigation Key Laboratory of Sichuan Province, Sichuan University, Chengdu 610065, China

(Received July 26, 2014, Revised January 25, 2016, Accepted February 19, 2016)

Abstract. This paper presents numerical modeling of the structural behavior of CFRP (carbon fiber reinforced polymer) strengthened RC (reinforced concrete) beams under four-point bending. Simulation of debonding at the CFRP-concrete interface was focused, as it is the main failure mode of CFRP strengthened RC beams. Here, cohesive layer was employed to model the onset of debonding, which further helps to describe the post debonding behavior of the CFRP strengthened RC beam. In addition, the XFEM approach was applied to investigate the effects of crack localization on strain field on CFRP sheet and rebar. The strains obtained from the XFEM correlate better to the test results than that from CDP (concrete damaged plasticity) model. However, there is a large discrepancy between the experimental and simulated load-displacement relationships, which is due to the simplification of concrete constitutive law.

Keywords: ABAQUS; reinforced concrete; CFRP strengthening; debonding; XFEM

1. Introduction

Numerical simulation on concrete structures (including strengthening forms) has been suffering from many shortcomings in constitutive theory, failure criteria, reinforcement, crack propagation as well as cohesive behavior (Ortiz 1985, Chaudhari *et al.* 2012, Zhou 2007, Wang 2007, Ozbakkaloglu *et al.* 2013). The commercial finite element codes, such as ABAQUS and ANSYS, are usually used to tackle the problems on modeling structural response of reinforced concrete, with appropriate constitutive relationships and failure criteria for specified conditions. The most popular models applied to simulate static and quasi-static behavior of concrete are Drucker-Prager (DP) model and Concrete Damaged Plasticity (CDP) model (Jiang *et al.* 2011, Wei *et al.* 2012, Bulent *et al.* 2010, Kmiecik *et al.* 2011). The DP model has some limitations in simulating FRP strengthened concrete structures due to lack of some essential features, which needs some modifications (Yu *et al.* 2010). Further more, the yield surface in the stress space requires retraction in modeling softening behavior which is incapable of simulating the degradation of elastic stiffness after concrete damage occurs. The limitations mentioned above can be overcome

*Corresponding author, Professor, E-mail: wangqy@scu.edu.cn

^aPh.D. Student, E-mail: xurichusheng1982@163.com

Table 1 Material properties

Material	Dimensions (mm)	f_c (MPa)	f_y (MPa)	f_u (MPa)	E (GPa)	η (%)
Concrete	C20	22.8	-	-	-	-
	C30	31.3	-	-	-	-
Steel bar	D=6	-	240	420	210	30
	D=8	-	330	490	210	28
	D=10	-	340	480	210	28
	D=14	-	410	555	200	28.5
CFRP	tf=0.111	-	-	4103	242	1.7

by CDP model (Yu *et al.* 2010, Yu *et al.* 2009).

Numerical studies on FRP-concrete bonded interface have been performed extensively (Pizhong *et al.* 2008, Biolzi *et al.* 2013, Lu *et al.* 2006, Coronado *et al.* 2006). In these studies, the failure of the cohesive material is assumed to follow a triangular curve in traction-separation relationship (Qiao *et al.* 2008, Diehl 2005). Tao *et al.* (2014) proposed a simple but robust FE model for simulating the debonding process for the single shear test, which agreed with test results. Sometimes, the tensile response of the cohesive material is directly extrapolated to shear response (Diehl 2005). This simplification may obtain an acceptable result under certain conditions, but care must be taken when using this simple assumption. This approach is hardly capable of predicting structures behavior. In the code ABAQUS, there is another way to treat the behavior of bonded surface which defines the contact properties of two surfaces (Fan *et al.* 2011). However, this method has little direct correlation to physical properties that are obtained through basic material tests. Therefore, only the cohesive layer approach was used herein.

Cracks initiation and propagation is still a challenging problem in numerical studies, as the majority of numerical models homogenized the effect of cracks in concrete structures including the CDP model. Thus the extended finite element method (XFEM) was developed (Sukumar *et al.* 2003, Roth *et al.* 2011, Zhang *et al.* 2013, Golewski *et al.* 2012). In the present study, the XFEM was applied to study the structural response of CFRP strengthened concrete beams. Here, the advantages and disadvantages of this method is discussed.

2. Experimental test

The experimental work was conducted by Dong *et al.* (2013), through which the enhancement of CFRP sheets on flexural and flexural-shear strengthening to RC beams was investigated. Details of the work will be described as follows.

2.1 Material

The ingredients of concrete used were 32.5R ordinary Portland cement, natural sand, gravels with aggregates size between 10 and 31 mm and water. Two concrete compressive strength were obtained based on two pouring method, C20 and C30, from cube crush tests. Table 1 shows the basic material properties of concrete, as well as that of steel rebar and CFRP sheet. The elastic

Table 2 Test results of beams with flexural strengthening

Beam	Crack load (kN)	Ultimate load (kN)	Deflection (mm)	Failure modes*
CR1	27.66	54.30	4.00	A
CR2	31.56	76.93	22.41	B
SR3	52.05	146.20	16.55	B

*Failure mode: A represents flexural failure, B represents CFRP debonding and flexural failure

modulus of concrete was calculated by applying an equation from the code for design of concrete structures of China (Design code 2010)

$$E_c = 100 / (2.2 + 34.7 / f_{cu}) \quad (1)$$

The calculated elastic modulus of C20 and C30 concretes were 26.87 GPa and 30.22 GPa, respectively.

2.2 Specimen and loading

Fig. 3 shows the strengthening methods of RC beams and loading and boundary conditions, whereas the corresponding mechanical properties are listed in Table 1.

2.3 Test results

The control beam showed classical flexural failure under four-point bending, i.e., cracks occurred at the center of bottom and propagated upwards. After flexural strengthening, the critical load to generate cracks increased, and the width of and space between cracks decreased. The failure mode was snapping and debonding of CFRP sheets.

From the test results, it is clear that the stiffness, failure deflection and ultimate load increased significantly, especially the ultimate deflection. The factors which influence the strengthening include number of CFRP sheets, pre-crack width and reinforcement ratio. Here, the stiffness of RC beam increased enormously with number of CFRP sheets, whilst the ultimate load was more dependent on reinforcement ratio than the depth of concrete cover thickness. Table 2 shows the improvement of CFRP strengthening on beam, which is also studied in this paper through numerical modelling.

3. Numerical modelling

3.1 Reinforced concrete model

3.1.1 Concrete model

The concrete damaged plasticity model (CDP) available in ABAQUS was used to simulate the behavior of the RC beam which can be referenced from extensive simulation work (Chaudhari *et al.* 2012, Mercan *et al.* 2010, Yu *et al.* 2010, Sinaei *et al.* 2012 and Burgers 2006). The CDP model assumes that the failure in both tensile cracking and compressive crushing of concrete is characterized by damage plasticity. Five basic parameters are required in CDP model, i.e., (1) the

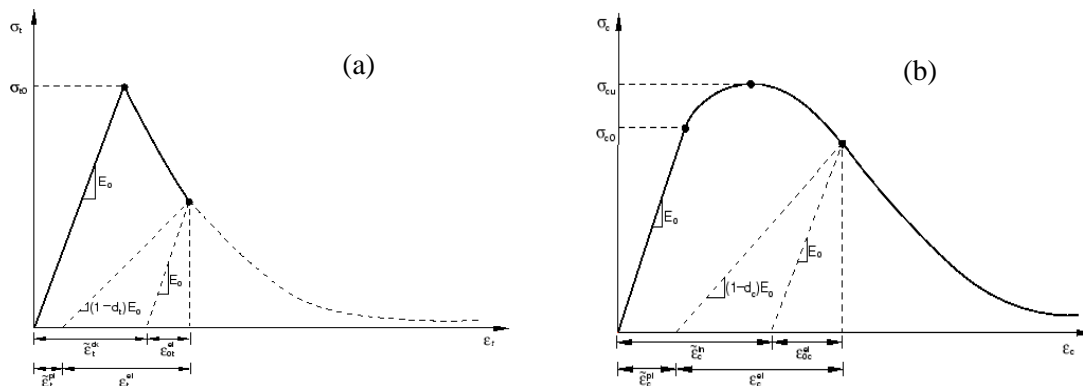


Fig. 1 Uniaxial stress-strain curve with damage in (a) tension and (b) compression

dilation angle in degrees, (2) the flow potential eccentricity, (3) the ratio of initial equibiaxial compressive yield stress to initial uniaxial compressive yield stress, (4) the viscosity parameter and (5) the ratio of the second stress invariant on the tensile meridian to that on the compressive meridian. Their default values are 33° , 0.1, 1.16, 0.67, and 0, which were used in the current study. As for the damaged behavior, Fig. 1 shows the stress-strain curves used in CDP theory, which defines the strain hardening and tensile softening behavior of concrete material, as well as the initiation and evolution of damage.

The tensile fracture and compressive plastic behavior are simulated by specifying the evolution laws of damage which represents the stiffness degradation. The damage variable “ d ” varies between 0 (representing no damage) and 1 (representing complete failure). The tensile damage variable d_t is assumed to be calculated by

$$d_t = 1 - \frac{\sigma}{f_c} \quad (2)$$

where σ is the traction related to COD (crack opening displacement) in the softening range. It is implemented in ABAQUS by using the keyword *CONCRETE TENSION DAMAGE, TYPE=DISPLACEMENT.

As the compressive stress in the beam under bending is always smaller than the compressive strength when tensile failure occurs, no compressive damage variables are needed.

The stress-strain curve of concrete shown in Fig. 1 can be obtained through tensile and compressive tests on concrete specimens. However, the tensile stress-strain relationship often introduce unreasonable mesh sensitivity into the results as the cracks localize in one or several elements’ width (Chen *et al.* 2011). To avoid this problem, Hillerborg’s fracture energy proposal is generally applied to allay this concern for many practical purposes, with which the concrete behavior is characterized by a stress-displacement (the displacement means crack opening displacement, COD) response rather than a stress-strain response. This is implemented in ABAQUS by using the keyword *CONCRETE TENSION STIFFENING, TYPE=DISPLACEMENT. The concrete in compression is modeled using the keyword *CONCRETE COMPRESSION HARDENING, TYPE=STRAIN. It should be noted that the strain and COD obtained from experimental tests include elastic parts but inelastic quantities are used in ABAQUS. Thus transformation is needed, i.e., getting inelastic strain by subtracting elastic

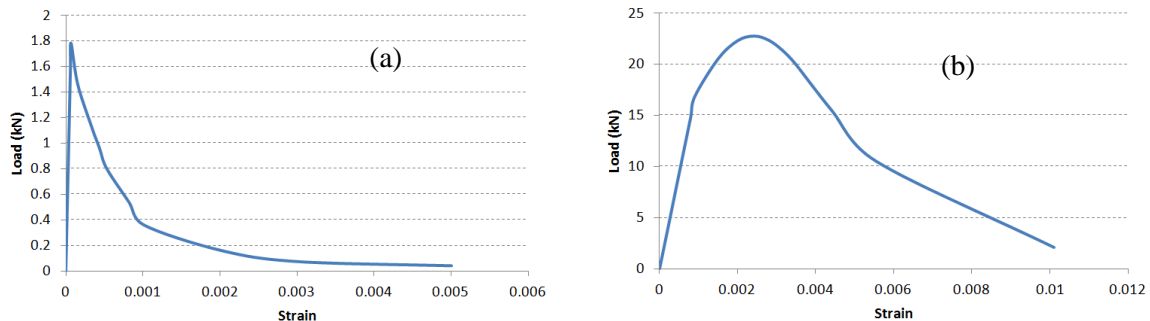


Fig. 2 Stress-strain curves from lab tests in (a) tension and (b) compression

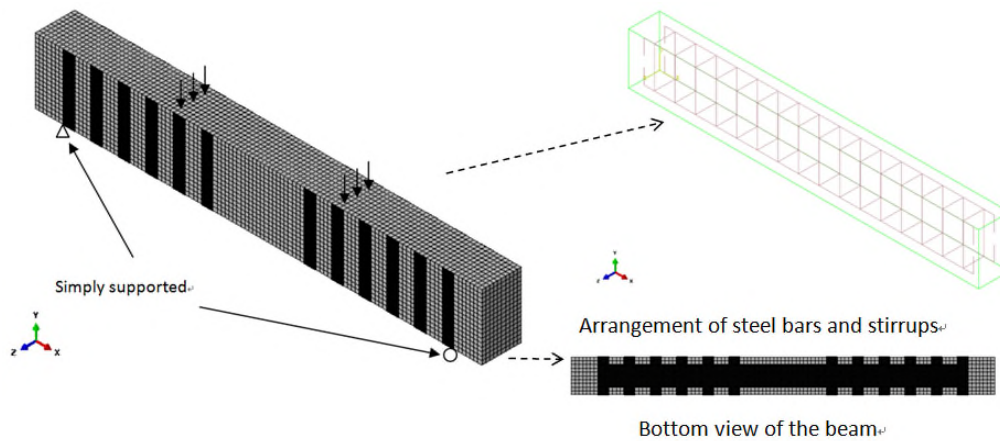


Fig. 3 Loading and boundary conditions

strain from total strain.

Fig. 2 shows the calculated stress-strain curves based on compressive strength since there is no test data. Generally, concrete behaves in a manner like curves shown in Fig. 1, and strength and strain at maximum stress are the two key points in stress-strain curve. The compressive strength was listed in Table 1 and the elastic modulus was calculated through Eq. (1).

3.1.2 Reinforcement of concrete

The tensile rebars and stirrups can be embedded into concrete body in ABAQUS simply by applying “embedded” constraint method. Fig. 3 shows the configuration of rebar and stirrups in concrete beam.

The rebar is often modeled as an elasto-plastic material, which can be referred to Table 1. The interaction between rebar and concrete is realized by defining the tension stiffening. Tension stiffening must be defined if concrete damaged plasticity model is applied, which can be specified by post-failure (failure stress is the stress at the onset of the damage initiation) stress-strain relationship (Sokolov 2010). The post-failure stress is often expressed as a function of crack strain. In order to guarantee the convergence of simulation, ABAQUS compels a floor level of stress that is 1/100 of the failure stress.

It is beneficial to convergence if every concrete element contains rebar element. Also

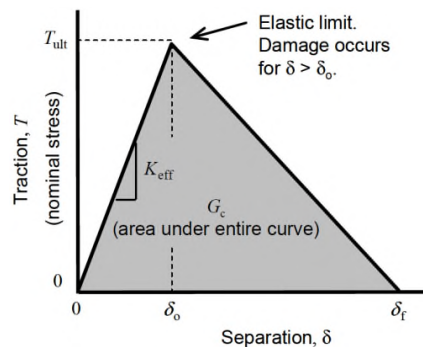


Fig. 4 ABAQUS traction-separation law for cohesive material

appropriate tension stiffening can reduce the mesh sensitivity of interaction between rebar and concrete. Therefore, estimation of tension stiffening is of high significance, which may be dependent on reinforcement ratio, cohesive strength between rebar and concrete, the size of aggregates and mesh density. One can make an assumption that the softening curve decreases linearly from failure stress point, and the strain at the end of softening curve is ten times of the strain at failure stress point which is 10^{-4} for a standard concrete. Therefore, when strain reaches 10^{-3} , the softening stress reaches zero.

The concrete beam was modeled by 8-node 3-D stress element with reduced integration (C3D8R), and reinforcing rebars by 2-node linear 3-D truss element (T3D2). The cross-section area of rebar was defined as a section property in property module of ABAQUS.

3.2 CFRP

Although CFRP sheet is an orthotropic material (much higher modulus and strength in woven directions than through the thickness directions), however within the plane it may be modeled as an isotropic material. This is because the loading on the CFRP sheet is stretching within the sheet plane.

3.3 Bonding

The CDP is suitable for reinforced concrete beam studied here, however the adhesion between CFRP sheets and concrete surface is of some complexity. Bulk material properties of adhesive are often unknown or not applicable to numerical analysis, and the physical thickness of adhesive is extremely small which is often considered to be “zero” in ABAQUS. Here, the traction-separation constitutive law relating stresses to separations in the through-thickness and transverse shear directions is employed. Fig. 4 shows the general form of the traction-separation law for cohesive element in ABAQUS. It should be pointed out that the law applies the bond separation distance instead of strain, which is formulated to represent the case of “zero” thickness bond. The basic concept in the cohesive element approach is that the cohesive elements carry loads to constrain the two parts together until loads and deformations on the cohesive elements cause damage and failure. When element has fully failed, it will release an amount of energy equal to the critical fracture energy obtained from material tests. To accommodate this within a finite element framework, the cohesive material must have finite definitions of stress and separation over which

the fracture energy can be released. For the triangular law used by ABAQUS, the cohesive element exhibits recoverable linear elastic behavior until the tensile separation reaches δ_0 , beyond which damage occurs and ultimately element fails, if the separation exceeds the material's failure separation, δ_f , which is referred as the cohesive ductility (Diehl 2005).

In fact, we cannot achieve an exact simulation of the separation with the cohesive element approach. Because the bond behaves infinitely rigid until it releases energy upon crack growth, thus the cohesive ductility δ_f is defined. Furthermore, the thickness of adhesion is assumed as zero. However, if the cohesive ductility is set too small, numerical problems will arise. A normal way to determine the value of δ_f is to multiplying the typical cohesive element mesh dimension by 0.05 (Diehl 2005). Therefore, all the 11 parameters (App. A) needed by the cohesive approach are not directly obtained from experiments. That means only the critical fracture energies are obtained from double cantilever beam test and end-notched flexural specimen test, and others are specified from theoretical approaches. After experimental test, the fracture energies was obtained as about 125 J/m².

The effective ultimate nominal stress T_{ult} of material and cohesive ductility (failure separation) δ_f are related to the critical fracture energy in the triangular traction-separation law via

$$G_c = \frac{T_{ult} \delta_f}{2} \quad (3)$$

Note that the cohesive ductility was assumed to be 0.05 times of the cohesive element size. Thus, the effective ultimate nominal stress T_{ult} of the bond material can be computed through Eq. (3). This is not the real ultimate stress of a bulk version of the bond material, but simply a penalty parameter.

Then, the initial elastic behavior of the cohesive material must be defined. From Fig. 4, the initial material stiffness per unit area (load per unit displacement per unit area), K_{eff} , is simply expressed as

$$K_{eff} = \frac{T_{ult}}{\delta_0} \quad (4)$$

The damage initiation ratio is defined as

$$\delta_{ratio} = \frac{\delta_0}{\delta_f} \quad (5)$$

δ_{ratio} is a simple scalar variable ranging between 0 and 1 used to define when damage initiates, which is often assumed to be 0.5. Combining Eqs. (3)-(5) there is

$$K_{eff} = \frac{2G_c}{\delta_{ratio} \delta_f^2} \quad (6)$$

$$E_{eff} = K_{eff} h_{eff} \quad (7)$$

The value of the effective elastic modulus of the cohesive material, E_{eff} , is related to K_{eff} via where h_{eff} is the initial effective thickness of the cohesive element. The user has two options of

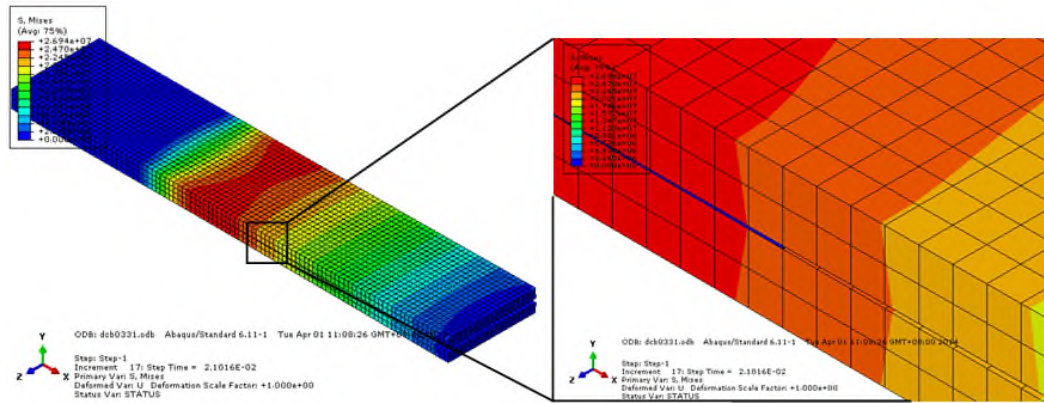


Fig. 5 Debonding of DCB specimen simulated

how this thickness is defined. One option is to have it defined by the actual geometric thickness by the nodal definitions defining the cohesive element (via `*COHESIVE SECTION, THICKNESS= GEOMETRY`). For many surface bonding applications this approach is highly problematic because the actual physical thickness of the bond (or bond material) is ill-defined or unknown. Another option is to define the geometric thickness (via nodal locations or orphan mesh offset method) as zero and then to manually define a constitutive thickness. A useful technique is to specify a unity thickness in this case (considering the actual thickness is often ill-defined). This means that the effective modulus is actually the initial cohesive material stiffness per unit area. It also means that the strains reported in the output database for the cohesive elements are actually the separation values.

Assuming a damage initiation ratio $\delta_{ratio} = 0.5$ and utilizing Eqs. (6)-(7), the effective elastic modulus, E_{eff} , can be computed.

Lastly, upon complete material failure of a given cohesive element, it is desirable to direct the code to remove the failed element from the solution.

Allowing failed cohesive elements to remain in the solution frequently created large numerical distortions caused by improper application of bulk viscosity damping on failed elements. This problem has been identified and will be addressed in future. Deleting the failed elements avoids ill effects on any of the solutions.

Fig. 5 shows the simulation result of DCB specimen, the blue line in the zoomed area indicates that the cohesive elements was still carrying loads while those disappeared had lost load carrying capacity.

3.4 Bonding arrangement

Orphan mesh method was used to fulfill cohesive approach. After mesh sensitivity examination, the mesh sizes of RC beam elements (10080 elements including concrete mesh and rebars mesh) were determined and the concrete mesh was imported as orphan mesh, then the rebars with determined mesh size were embedded into concrete orphan mesh.

The cohesive elements were offset from concrete orphan mesh from expected place with a thickness of zero, while the CFRP sheets elements were offset from cohesive elements with a finite thickness.

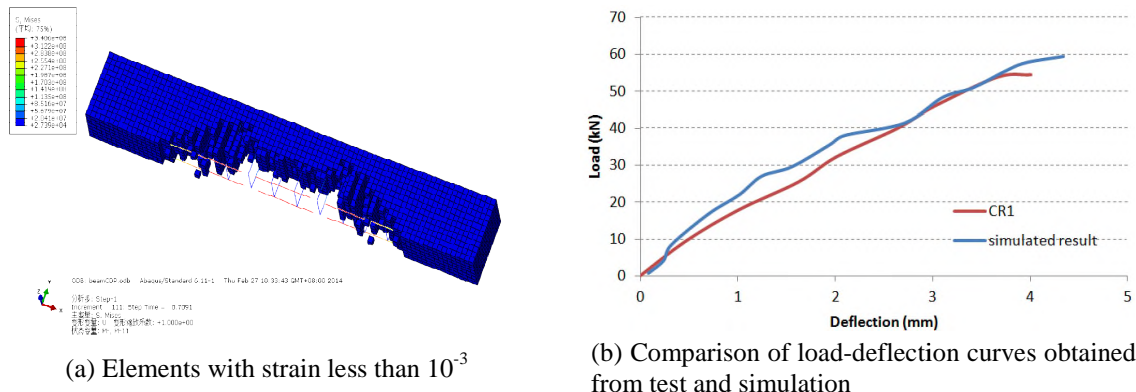


Fig. 6 Simulated result of the control beam

In case that the edge of CFRP sheets come off firstly (function of U-shaped CFRP sheets in flexural strengthening method used by Dong *et al.* 2013), strips of cohesive elements with extremely high strength (high enough to maintain bonding from beginning to end) were assigned at CFRP sheet edges.

3.5 XFEM method

In order to investigate effects of localized cracks on the response of CFRP sheets strengthened RC beam, the XFEM model was applied. However, the CDP model cannot be used since a cracking stress must be defined in the XFEM model. In this case, the constitutive law of concrete must be simplified as a linear elastic fracture material. Flexural strengthened RC beam was simulated by the XFEM model.

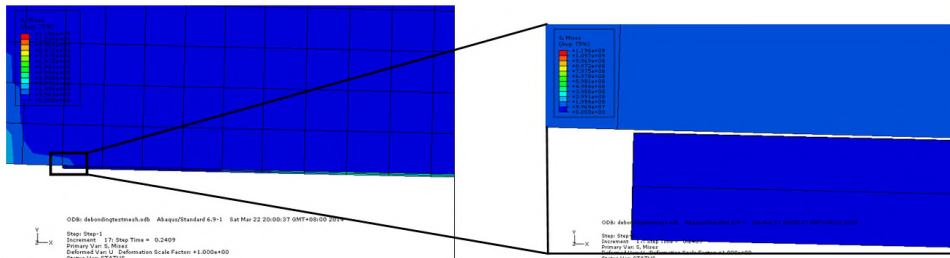
To be able to compute cracks using XFEM in ABAQUS, a few simple steps are needed: a crack must be defined, the crack domain must be chosen, and the output of interest is specified. These steps are explained below according to ABAQUS 6.11 Online Documentation. The crack is created as a shell surface for 3D cases and positioned as desired (bottom of the vertical symmetry plane in present model). ABAQUS automatically finds the positioning of the crack in the solid model using the Level set method. The Level set method defines the crack face and the crack front. The isoplane is called PHILSM in ABAQUS and needs to be selected in the Field output requests to be able to visualize the crack opening in the post-process.

The crack domain defines where the enrichment features can be added to the finite element approximation, i.e., the region where a crack can be described with XFEM. It is specified manually and for stationary crack analyses it must contain any existing crack.

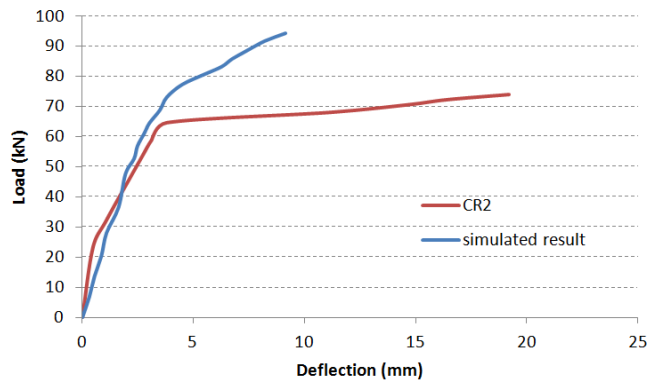
4. Simulation results and discussion

4.1 Results of control beam

Fig. 6(a) shows the concrete element with tensile strain less than 10^{-3} , and Fig. 6(b) shows the load-displacement curve of the control beam compared with test results (the test result was

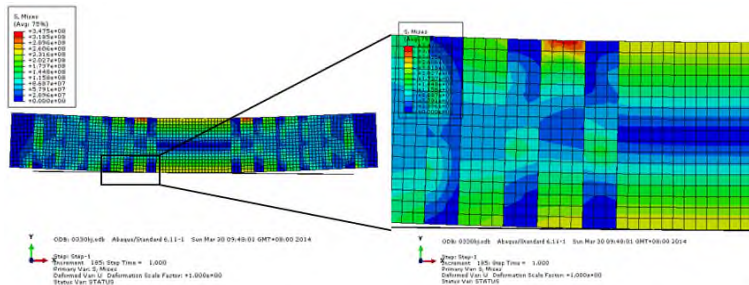


(a) Debonding failure of CFRP

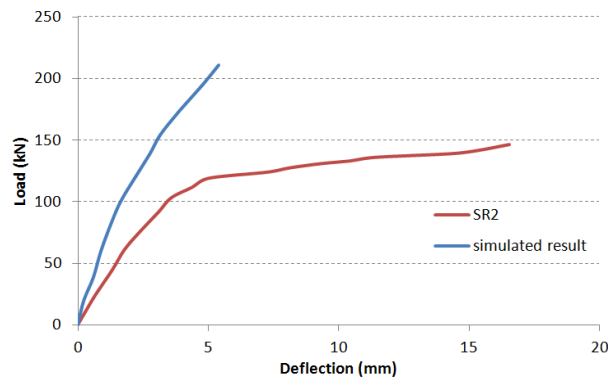


(b) Comparison of load-deflection curves obtained from test and simulation

Fig. 7 Simulated result of flexural strengthened beam CR2

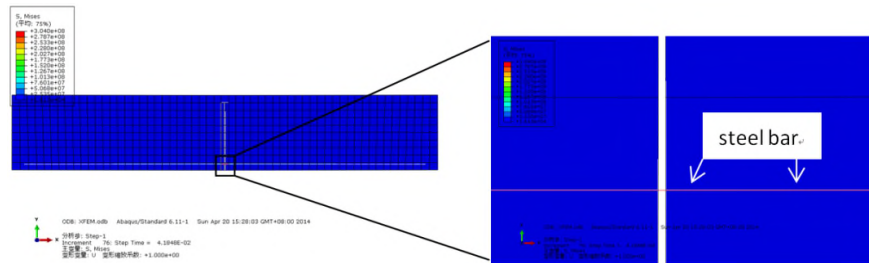


(a) Snapping failure of CFRP

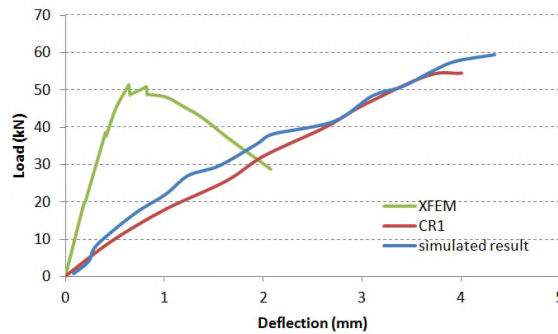


(b) Comparison of load-deflection curves obtained from test and simulation

Fig. 8 Simulated result of flexural-shear strengthened beam SR2



(a) Crack propagated by using XFEM



(b) Load-deflection curves obtained from XFEM

Fig. 9 Simulated results by XFEM method

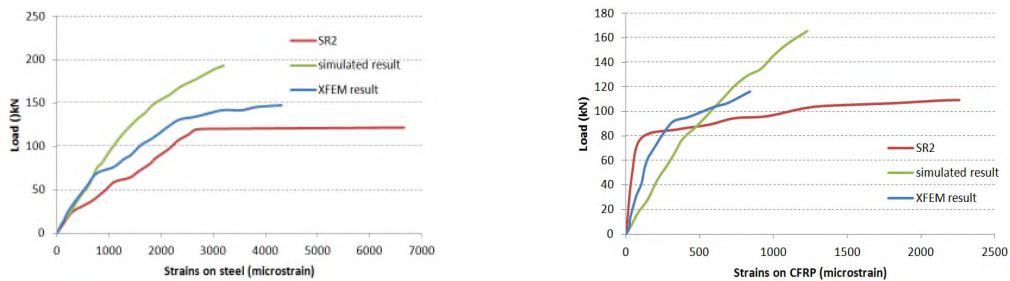


Fig. 10 Simulated strain results of flexural-shear strengthened beam SR2

labeled by beam serial number which was adopted hereinafter). From Fig. 6(a) it can be seen that at step time of 0.71, i.e., equivalent to 71% of the applied load, the failure elements passed through the middle depth of the beam, which means the RC beam lost its loading capacity. The load and deflection at this moment are 58.29 kN and 4.14 mm, respectively, which correlate to the test results (54.30 kN and 4.00 mm) reasonably well.

4.2 Results of CFRP strengthened beam

4.2.1 Failure mode

Fig. 7 shows the simulated results of the flexurally strengthened beam CR2, and Fig. 8 shows that of flexural-shear strengthened beam SR2. The agreement between experimental data and numerical results was kept at the early stage of the curve, but it was not the case as load increased.

This is because the flexural failure of RC beam in numerical model was “averaged” to the whole body while there were cracks with finite width propagated from mid-bottom of RC beam in actual condition. Crack width can reduce the flexural stiffness of RC beam, and that is why the numerical modeling over estimates the stiffness of the experimental one after the load exceeds a certain value. Furthermore, the same problems also happened to strains that will be discussed later.

4.2.2 The XFEM method

The XFEM method was applied to take crack propagation into consideration, and simulated result was shown in Fig. 9. The accuracy of the predicted element strains was improved, as shown in Fig. 10, in comparison to the response of the concrete beam deviated from its CDP model.

However, the load-deflection relationship for RC beam is predicted far away from test result (Fig. 9(b)) by XFEM method. This is due to the simplification of concrete constitutive relation in the XFEM method since CDP model is incompatible with XFEM method.

5. Conclusions

Concrete damaged plasticity model can be used to predict the behavior of concrete well in case that the tensile and compressive stress-strain relationships can be obtained. However, it is unable to reflect the localized crack initiation and propagation since it “averaged” the damage of concrete. Therefore, the CDP model is not suitable for concrete structures with localized cracks, such as CFRP strengthened RC beam studied in this paper. The extended finite element method (XFEM) can be used to simulate crack propagation in structures under simple conditions, but the constitutive relations of concrete based on the XFEM in ABAQUS still needs further development. Looking into recent studies on concrete constitutive laws, one would want to develop the XFEM on concrete from meso-mechanics point of view.

ABAQUS is capable of simulating surface interaction behavior not only through directly defining bond material properties, interface contact properties is another effective method to fulfill this task. When defining bond material properties, a few parameters cannot be obtained from tests, instead they are the theoretical values calculated based on the critical fracture energy G_c .

Acknowledgements

This work was supported by the National Natural Science Foundation of China (Grant No. 51408382) and the Science and Technology Supported Program of Sichuan (Grant No. 2015GZ0245).

References

- Abaqus Analysis User's Manual 6.11.
- Biolzi, L., Ghittoni, C., Fedele, R. and Rosati, G. (2013), “Experimental and theoretical issues in FRP-concrete bonding”, *Constr. Build. Mater.*, **41**, 182-190.
- Burgers, R. (2006), “Non-linear FEM modelling of steel fibre reinforced concrete”, Report, Delft University of Technology, Delft.

- Carlos, A., Maria, C. and Lopez, M. (2006), "Sensitivity analysis of reinforced concrete beams strengthened with FRP laminates", *Cement Concrete Compos.*, **28**(1), 102-114.
- Chaudhari, S.V. and Chakrabarti, M.A. (2012), "Modeling of concrete for nonlinear analysis using finite element code ABAQUS", *Int. J. Comput. Appl.*, **44**(7), 14-18.
- Chen, J.F. and Tao, Y. (2011), *Finite element modeling of FRP-to-concrete bond behavior using the concrete damage plasticity theory combined with a plastic degradation model*, Springer-Verlag, **45**.
- Design code (2010), *Code for design of concrete structures*, China.
- Diehl, T. (2005), "Modeling surface-bonded structures with ABAQUS cohesive elements: beam-type solutions", ABAQUS Users' Conference.
- Dong, J., Wang, Q. and Guan, Z. (2013), "Structural behavior of RC beams with external flexural and flexural-shear strengthening by FRP sheets", *Compos. Part B*, **44**(1), 604-612.
- Fan, J., Guan, Z.W. and Cantwell, W.J. (2011), "Numerical modelling of perforation failure in fibre metal laminates subjected to low velocity impact loading", *Compos. Struct.*, **93**(9), 2430-2436.
- Foraboschi, P. (2014), "Predictive multiscale model of delayed debonding for concrete members with adhesively bonded external reinforcement", *Compos. Mech., Comput., Appl.*, **3**(4), 307-329.
- Golewski, G.L., Golewski, P. and Sadowski, T. (2012), "Numerical modelling crack propagation under Mode II fracture in plain concrete containing siliceous fly-ash additive using XFEM method", *Comput. Mater. Sci.*, **62**, 75-78.
- Jiang, J., Wu, Y. and Zhao, X. (2011), "Application of drucker-prager plasticity model for stress-strain modeling of FRP confined concrete columns", *Procedia Eng.*, **14**, 678-694.
- Kmiecik, P. and Kaminski, M. (2011), "Modeling of reinforced concrete structures and composite structures with concrete strength degradation taken into consideration", *Arch. Civil Mech. Eng.*, **6**(3), 623-636.
- Li, W., Li, Q. and Jiang, W. (2012), "Parameter study on composite frames consisting of steel beams and reinforced concrete columns", *J. Constr. Steel Res.*, **77**, 145-162.
- Lu, X.Z., Jiang, J.J., Teng, J.G. and Ye, L.P. (2006), "Finite element simulation of debonding in FRP-to-concrete bonded joints", *Constr. Build. Mater.*, **20**(6), 412-424.
- Mercan, B., Schultz, A.E. and Stolarski, H.K. (2010), "Finite element modeling of prestressed concrete spandrel beams", *Eng. Struct.*, **32**(9), 2804-2813.
- Ortiz, M. (1985), "A constitutive theory for the inelastic behavior of concrete", *Mech. Mater.*, **4**(1), 67-93.
- Ozbakkaloglu, T., Lim, J.C. and Vincent, T. (2013), "FRP-confined concrete in circular sections: Review and assessment of stress-strain models", *Eng. Struct.*, **49**, 1068-1088.
- Qiao, P. and Chen, Y. (2008), "Cohesive fracture simulation and failure modes of FRP-concrete bonded interfaces", *Theor. Appl. Fract. Mech.*, **49**(2), 213-225.
- Roth, S.N., Leger, P. and Soulaïmani, A. (2011), "XFEM using a non linear fracture mechanics approach for concrete crack propagation in dam safety assessment", *Proceedings of the 8th International Conference on Fracture Mechanics of Concrete and Concrete Structures*.
- Sinaei, H., Shariati, M., Abna, A.H., Aghaei, M. and Shariati, A. (2012), "Evaluation of reinforced concrete beam behavior using finite element analysis by ABAQUS", *Sci. Res. Essay.*, **7**(21), 2002-2009.
- Sokolov, A. (2010), "Tension stiffening model for reinforced concrete beams", Ph.D. Dissertation, Vilnius Gediminas Technical University, Vilnius.
- Sukumar, N. and Prévost, J.H. (2003), "Modeling quasi-static crack growth with the extended finite element method Part I: Computer implementation", *Int. J. Solid. Struct.*, **40**(26), 7513-7537.
- Wang, Z. (2007), "The fracture and bond performances of fiber reinforced and rehabilitated concrete", Ph.D. Dissertation, Zhengzhou University, Zhengzhou.
- Yu, T., Teng, J.G., Wong, Y.L. and Dong, S.L. (2010), "Finite element modeling of confined concrete-I: Drucker-Prager type plasticity model", *Eng. Struct.*, **32**(3), 665-679.
- Yu, T., Teng, J.G., Wong, Y.L. and Dong, S.L. (2010), "Finite element modeling of confined concrete-II: Plastic-damage model", *Eng. Struct.*, **32**(3), 680-691.
- Zhang, S., Wang, G. and Yu, X. (2013), "Seismic cracking analysis of concrete gravity dams with initial cracks using the extended finite element method", *Eng. Struct.*, **56**, 528-543.
- Zheng, Y., Robinson, D., Taylor, S. and Cleland, D. (2009), "Finite element investigation of the structural

behaviour of deck slabs in composite bridges”, *Eng. Struct.*, **31**(8), 1762-1776.
Zhou, S. (2007), “The numerical simulation and meso-mechanics analysis of the concrete damage process in the static and dynamic loads”, Ph.D. Dissertation, Xi’an University of Technology, Xi’an.

CC

Appendix A

The cohesive model in ABAQUS requires 11 input parameters which are as follows (partly optional):

*ELASTIC, TYPE=TRACTION

Eeff, Eeff, Eeff

*DAMAGE INITIATION, CRITERION=MAXS

Tult, Tult, Tult

*DAMAGE EVOLUTION, TYPE=ENERGY, MIXED MODE BEHAVIOR=BK, POWER=n

G_{Ic} , G_{IIc} , G_{IIIc}

*COHESIVE SECTION, RESPONSE=TRACTION SEPARATION,

THICKNESS=SPECIFIED, 1.0

